applied sciences

MDPI

Article

Design and Simulation of the Robust ABS and ESP Fuzzy Logic Controller on the Complex Braking Maneuvers

Andrei Aksjonov [1,2,*], Klaus Augsburg [2] and Valery Vodovozov [1]

[1] Faculty of Power Engineering, Tallinn University of Technology, Tallinn 12616, Estonia; valery.vodovozov@ttu.ee

[2] Department of Mechanical Engineering, Technische Universität Ilmenau, Ilmenau 98693, Germany; klaus.augsburg@tu-ilmenau.de

* Correspondence: andrei.aksjonov@ttu.ee; Tel.: +49-157-8899-8333

Academic Editor: Arun Somani

Received: 5 September 2016; Accepted: 17 November 2016; Published: 25 November 2016

Abstract: Automotive driving safety systems such as an anti-lock braking system (ABS) and an electronic stability program (ESP) assist drivers in controlling the vehicle to avoid road accidents. In this paper, ABS and the ESP, based on the fuzzy logic theory, are integrated for vehicle stability control in complex braking maneuvers. The proposed control algorithm is implemented for a sport utility vehicle (SUV) and investigated for braking on different surfaces. The results obtained for the vehicle software simulator confirm the robustness of the developed control strategy for a variety of road profiles and surfaces.

Keywords: energy-efficient computing; fuzzy control; high-performance computer systems; road vehicles; vehicle safety

1. Introduction

The rapidly growing demand for passenger and commercial vehicles increases the number of road accidents around the world. In addition to their negative influence on road safety, accidents also have an indirect harmful impact on the environment and cause threats to human health and life. In cases when the human factor plays an important role, modern electronics and control systems may support the driver's reaction and skills to improve the stability and performance of the vehicle and avoid accidents. Two of the most important on-board safety systems are ABS and ESP. Both systems have become mandatory for all passenger vehicles and most commercial vehicles. The ABS and ESP safety features in vehicle dynamics control have been known for a long time. However, the existing control algorithms are rarely investigated from the viewpoint of robust operation in different road conditions. Many of the results discussed in the published studies are describing simple maneuvers, such as straight-line braking with a uniform road surface. Few investigations are known for emergency braking on complex road profiles, such as a curved road with split-μ or a curved road with varying tire–road friction coefficients.

Within the framework of the presented study, fuzzy theory has been selected for the controller implementation. The fuzzy logic controllers (FLC) are known as efficient tools in solving complex tasks such as ABS and ESP control. A combination of ABS and ESP can solve the robustness problem of the braking performance. To confirm it, the FLC-based braking will be discussed for the different complex maneuvers such as a combination of road profiles and split-μ road surfaces.

The first ABS applications arose several decades ago [1] and still use rule-based methods as the dominant control approach. In the modern ABS systems installed in commercial vehicles, the

braking pressure is increased or reduced based on the wheel speed and the slip switching threshold comparison [1]. The slip is set to a constant value, for instance 20% as it is optimal for the most common surface—dry asphalt. The braking surface is not recognized and the threshold value is equal for every road condition. This approach leads to energy losses because each road adhesive characteristic requires its optimal wheel slip value. This is why many researchers have focused on intelligent control algorithms for braking processes, trying to estimate an optimal one for every road condition slip threshold.

However, the analysis of the bibliography presented in [2] shows that nowadays the FLC is also being intensively used in ABS and ESP design. One of the first ABS control mechanisms based on the fuzzy algorithm was patented in 1989 by the Nissan Motor Co., Ltd., (Yokohama, Japan) [3]. Furthermore, many other solutions based on the FLC were proposed. Thanks to its simplicity and robustness, FLC proved to be equally applicable to on-road [4] and off-road vehicles [5].

In [6], a model reference adaptive control (MRAC) was introduced to tune the FLC in order to be able to control all kinds of nonlinear systems. Furthermore, the MRAC was used in a braking system in [7] as an ABS intelligent control. The simulation results were shown for a variety of road conditions (from icy to wet). The proposed solution requires a reference slip value, which is set to 20% for any kind of road surface. A similar assumption for the constant value of the optimal wheel slip is also proposed for ABS, as described in [8]. Another example is the model-based Takagi–Sugeno (T–S) FLC designed for a single-car model [9]. The controller copes well in optimal braking wheel slip maintenance, which the model considers a reference constant. Many different fuzzy proportional-integral-derivative (PID) approaches were also investigated [10–12]. Yet the results are limited because the situation considered in most cases is braking on a straight road with an optimal slip of 20%.

Adaptive and self-tuning intelligent FLC solutions have also been introduced in various studies [13,14]. In [15] a genetic neural FLC is designed, where the algorithm requires the reference wheel slip profile. The approach with the estimation of road parameters is used in [16], where various roads can be identified to keep the optimal slip by the controller. This controller demonstrated good performance but its operation was illustrated for simple straight braking maneuvers.

Many studies have presented the validation of fuzzy-based ABS algorithms through tests on a hardware-in-the-loop (HIL) experimental setup or ABS test bench connected to the real-time vehicle software simulator. For example, in [17] the authors introduced the fuzzy ABS with the road friction estimation algorithm. Consequently, the experiments were conducted for the variable road conditions proving the FLC robustness. In [18] the ABS algorithm holds the optimal wheel slip for different roads and is validated for quarter-car HIL systems.

For complex braking maneuvers on split-μ surfaces and curved roads the activation of the ESP system can be required. In this field, fuzzy logic methods are also finding wide application. For example, patents have been issued to FLC control algorithm, where yaw rate and steering wheel angle signals were considered the control inputs to maintain vehicle stability during braking [19]. Nevertheless, the described controller is still P or PD FLC, which requires the reference input.

In addition, many known examples are validated for specific maneuvers only. In particular, the PID FLC for yaw motion control [20,21] was investigated on double line maneuvers. The FLC neural network [22] shows the experimentation results conducted for split-μ straight road maneuvers. The T–S FLC [23] and fuzzy robust H∞ [24] methods were tested on line change maneuvers. The authors in [25] have integrated yaw moment and active front steering controllers based on the FLC. The results are demonstrated by the single line change maneuvers.

It should be noted that the use of simple maneuvers for the controller validation cannot demonstrate the FLC robustness. In reality, the driver deals with different road scenarios. Therefore, the controller applicability has to be studied on more complex and different braking maneuvers such as emergency braking on curved split-μ or variable road surfaces to assure controller robustness. Moreover, the reference slip direct control does not guarantee safety assistance on the split-μ surfaces as the steerability is not preserved. This issue must also be addressed.

As suggested in many previous studies, controllers as well as the currently installed systems in the vehicles set the slip value at 20% for any kind of roads. On the one hand, such an approach can be enough to maintain the steering ability. On the other hand, it leads to a decline in braking performance. For example, on average the optimal slip for icy roads is between 7% and 10%. Thus λ = 20% would cause a more than 50% loss of braking performance and the vehicle operation would become unstable, i.e., a diminution in steerability. Therefore, by holding the optimal wheel slip value and avoiding the controller restriction with reference variable, as it is proposed in the current paper, the effectiveness and energy efficiency of the braking process is maintained [1] (pp. 74–94).

This paper contributes to the advancement of ABS and brake-based ESP systems using FLC. In particular, the article describes the research results connected with the following topics:

- ESP and ABS control combination, both designed using fuzzy theory.
- Use of a 10 degrees-of-freedom (10 DOF) four-wheel vehicle model in the controller.
- Demonstration of the control robustness on different road surfaces and profiles.

The paper is organized as follows. The next section is dedicated to vehicle dynamics and model parameterization. Section 3 explains the FLC design. The Section 4 is devoted to the experimental facilities. Next, the simulation outcomes are provided. Conclusions are summarized in Section 6.

2. Vehicle Dynamics

2.1. Vehicle Model

The single-wheel model of the vehicle is shown in Figure 1a. The single-track (bicycle) model is introduced in Figure 1b. Table 1 introduces nomenclature for all variables used in these and other models mentioned in the paper.

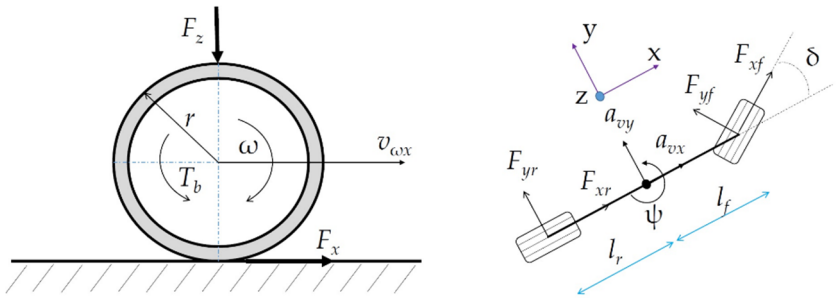

Figure 1. Vehicle model schematic drawing: (**a**) single-wheel model; (**b**) single-track model.

Single wheel dynamics can be expressed by the following equations:

$$I_{wi} \cdot \dot{\omega}_i = T_{ti} - r_i \cdot F_{xi} - T_{bi} \tag{1}$$

$$F_{xi} = m \cdot \dot{v}_{xi} \tag{2}$$

$$F_{zi} = m \cdot g. \tag{3}$$

Brake torque depends on the applied brake pressure:

$$T_{bi} = r_i \cdot k_b \cdot p_{bi}, \tag{4}$$

where k_b is the braking coefficient, which depends on the brake disc friction area, mechanical efficiency of the brake components, and the braking factor is the constant value. In this paper, the ABS controller output variable is the braking pressure for each wheel, p_{bi}.

The wheel slip at braking is calculated as follows:

$$\lambda_i = \frac{v_v - v_{wx\_i}}{v_v}. \tag{5}$$

The longitudinal wheel speed be can also simply calculated as:

$$v_{wx\_i} = r_i \cdot \omega_i. \tag{6}$$

Table 1. Parameters description.

Symbol	Description	Annotation
ω	Wheel angular speed [1]	rad/s
a_{vx}	Vehicle longitudinal acceleration [1]	m/s^2
a_{vy}	Vehicle lateral acceleration [1]	m/s^2
ψ	Yaw rate [1]	rad/s
δ	Steering wheel angle [1]	rad
p_b	Braking pressure [1]	bar
r	Wheel radius	m
m	Mass of the vehicle	g
g	Gravitational acceleration	m/s^2
T_b	Braking torque	Nm
T_t	Traction torque	Nm
k_b	Braking coefficient	-
v_{vx}	Vehicle longitudinal velocity	m/s
v_{wx}	Wheel longitudinal velocity	m/s
λ_i	Wheel slip	%
μ	Tire–road friction coefficient (general)	-
μ_x	Tire–road friction coefficient based on vehicle longitudinal acceleration	-
l_f	Distance from the vehicle Center of Gravity (COG) to the front axles	m
l_r	Distance from the vehicle COG to the rear axles	m
I_z	Yaw moment of inertia about z-axis	g·m^2
F_x	Longitudinal force	N
F_y	Lateral force	N
F_z	Vertical force	N
p_{ABS}	Pressure generated for ABS braking	bar
p_{ESPl}	Pressure generated for the yaw rate regulation for the left side wheels of the vehicle	bar
p_{ESPr}	Pressure generated for the yaw rate regulation for the right side wheels of the vehicle	bar
s	Distance	m
$-a_{average}$	Average deceleration	m/s^2
ABS_{IP}	ABS operation index of performance	-
λ_{average}	Average wheel slip value	%
$\omega_{\text{p-t-p}}$	ABS adaptability peak-to-peak value	%
i	Subscript for each wheel; $i \in$ [FL, FR, RL, RR] [2]	-

[1] Measured by the sensor; [2] (Front Left, Front Right, Rear Left, Rear Right).

In reality the tire radius r_i is a dynamic variable. In our case we simplify the equation and consider it as a constant value as the change in radius dimension is negligibly small.

The FLC design requires information about the friction-slip curves. Tire–road friction coefficient can be determined as follows:

$$\mu_x(\lambda) = \frac{F_x}{F_z}. \tag{7}$$

Using Equations (2) and (3), μ_x can be estimated:

$$\mu_x \approx \frac{\dot{v}_x}{g}. \tag{8}$$

The 3 DOF single-track model, 0b, is required for the formulation of control inputs in the case of vehicle maneuvers with lateral dynamics. The model is described by the following system of equations:

$$\begin{cases} m \cdot a_{vx} = F_{xf} \cdot \cos\delta + F_{xr} - F_{yf} \cdot \sin\delta + m \cdot \dot{y} \cdot \psi \\ m \cdot a_{vy} = F_{xf} \cdot \sin\delta + F_{yf} \cdot \cos\delta + F_{yr} - m \cdot \dot{x} \cdot \psi \\ \dot{\psi} \cdot I_z = l_f \left(F_{xf} \cdot \sin\delta + F_{yf} \cdot \cos\delta \right) - l_r \cdot F_{yr} \end{cases}. \tag{9}$$

2.2. Model and Controller Parameterization

Before the simulation, the vehicle model is parameterized according to the sport-utility vehicle. The parameters are taken from the vehicle manufacturer. The total mass is 2170.39 kg. The tires for each wheel are set Continental® (Hanover, Germany) 235/55 R19 and are modeled with Pacejka's tire magic formula, the coefficients are also provided by the tire manufacturer.

In order to set the initial parameterization of the FLCs, a specific case study was conducted first. The model was simulated under heavy braking conditions on different surfaces to obtain the wheel lock. The ABS and ESP control was not activated. During the case study simulation, the normalized traction/braking forces for every road condition with the locked wheels were evaluated. Therefore, the curves of the normalized traction/braking force of the tire μ versus the wheel slip λ for different road surfaces were built (Figure 2).

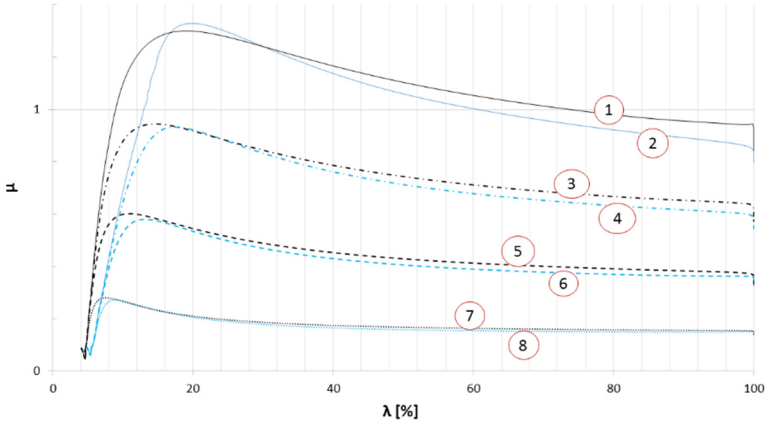

Figure 2. The μ versus λ curves for the different road surfaces for the studied vehicle model: 1—dry road rear wheels, 2—dry road front wheels, 3—damp road rear wheels, 4—damp road front wheels, 5—wet road rear wheels, 6—wet road front wheels, 7—icy road rear wheels, 8—icy road front wheels.

The stable area is where the curve grows from 0 by λ to its maximum value of μ. The second part of the curve is the unstable region, when the steering remains uncontrollable. Efficient ABS performance depends on the road surface. Each surface (dry, damp, wet, icy) has its own optimal slip while braking. The optimal slip refers to the top area of the curve where μ obtains its maximum value during braking (Figure 2), thus remaining stable. The optimal slip values for each curve, according to the plots in Figure 2, are presented in Table 2.

Table 2. Optimal wheel slip values for several road conditions.

λ (%)	Front Wheels	Rear Wheels
Dry road surface	19.85	18.96
Damp road surface	17.53	14.65
Wet road surface	13.21	10.88
Icy road surface	8.95	7.55

The plots are important for the FLC universe of discourse (UOD) design, to set the workspace for the slip input variables in order to guarantee the controller robustness. During the case study the workspace for friction coefficient was also investigated. In addition, the yaw rate UOD was explored in the case study for emergency braking.

3. Fuzzy Logic Control Design

When the dynamical behavior of the object is studied, the controller is ready to be designed. One of the advantages of the solution described in this paper is that the controller requires the input variables, for which signals are transmitted in real time by the sensors available in modern vehicles.

The fuzzy logic controller architecture is shown in Figure 3. In this case the plant is a vehicle model. The FLC consists of four design steps. Fuzzification is the process of converting the "crisp" (real number) input into fuzzy sets. A fuzzy set in turn is a pair consisting of an element in UOD and membership degree. The inference mechanism (engine) is used to turn the fuzzy input into a fuzzy output, using the composed rule-base block. Finally, defuzzification converts the fuzzy output into a numerical value.

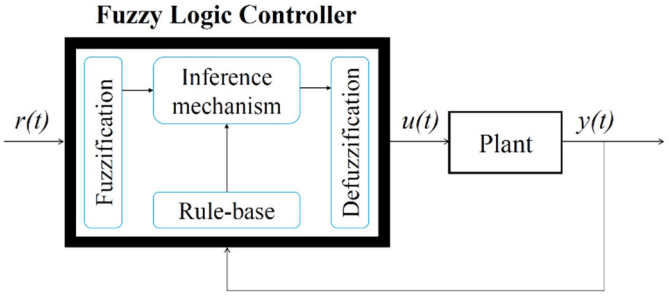

Figure 3. Fuzzy logic controller system block diagram: $r(t)$—reference input, $u(t)$—process inputs, $y(t)$—process.

The MATLAB® (Natick, MA, USA) Fuzzy Logic Toolbox™ is used to design the FLC. At the beginning, the inputs and outputs must be stated. Two separate FLCs for ABS and ESP are introduced and combined to obtain robust brake and stability control.

The block diagram scheme for a single wheel is presented in Figure 4. The anti-lock braking system controller involves longitudinal wheel speeds and vehicle acceleration. Using Equations (5) and (6), the slip for each wheel λ_i is calculated and the variable serves as an input. The second input is the tire–road friction coefficient, which corresponds to the vehicle body acceleration and is donated as μ_x, as stated in Equation (8).

The ABS is activated together with the braking pedal displacement. When the vehicle velocity is lower than 8 km/h, the ABS does not function because, after the vehicle speed of 8 km/h, the distance traveled with locked wheels is not critical. The activation requirements are taken from [1] (pp. 74–94).

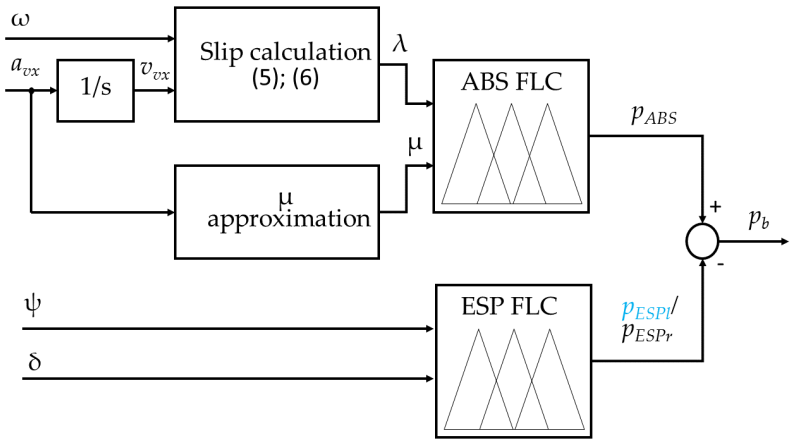

Figure 4. Controller block scheme for a single wheel: ABS FLC—anti-lock braking system fuzzy logic controller, ESP FLC—electronic stability program fuzzy logic controller, 1/s—integrational operation.

As soon as the emergency brake (full pedal actuation) is deployed, before the ABS is activated, the controller has enough time to measure the car's maximum deceleration and use it as a constant variable to understand the road surface. Moreover, the controller resets the μ_x variable every second and the maximum value of a_{vx} is measured again. The fast reset has no effect on driving comfort as the process is very rapid. The reset is necessary for the FLC to understand if the road condition has remained the same, for example, when the road changes from a dry to an icy surface.

The inputs of the ESP are the angular velocity of the vehicle about the vertical axis ψ and the steering wheel angle δ operated by the driver (Figure 4). The ESP is activated together with the braking pedal and deactivates when the vehicle speed is below 8 km/h.

The output of the ABS and the ESP is the braking pressure. The yaw controller has no impact when the yaw moment is not created, thus only ABS is responsible for efficient braking on a straight homogeneous road.

The ESP FLC controls both sides of the vehicle. It either regulates the right or left pair of the vehicle wheels, depending on the body yaw rate direction. According to the curves in Figure 2, the front and rear wheels require different optimal wheel slip values. Therefore, the front and rear wheels will have different membership functions (MFs) for the λ input in ABS. Consequently, each wheel has a different controller. When the yaw FLC understands that the driver is losing vehicle control, it reduces the braking pressure from the side of the car, in which direction the vehicle starts to spin around its center of gravity (COG). Otherwise, only the ABS control is operating.

The next step is to design membership functions for all the inputs and outputs (Figure 5). The linear (triangular) MFs were applied, which are characterized by fast reaction due to the narrow shape as compared to other MFs (exponential, quadratics).

The MFs are symmetrical to provide an equal sensitivity for the whole UOD and obtain the whole overlap of the UOD between the MFs. Each variable UOD must have a closed frontier between [*min*, *max*]. For the input variables, the bounds are obtained during the parameterization described in Section 2.

The slip input MFs for the ABS are introduced in Figure 5. There are nine MFs in total. The UOD for the front wheels lay between [0.08, 0.22]. This area is accepted according to the operational space obtained in Figure 2 for the front wheels. The only difference between the front and the rear wheels is that the UOD of the slip input for the last ones is accepted in a range [0.07, 0.2], which is also based on the rear slip curves in Figure 2 for the rear wheels. In short, UOD for the slip covers all stable areas for relevant roads.

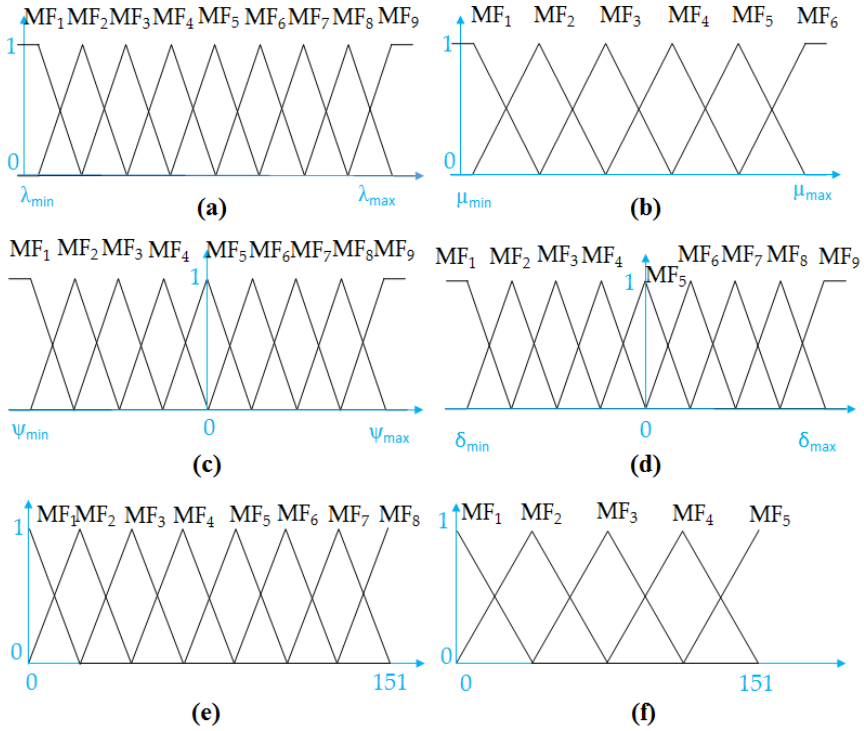

Figure 5. Fuzzy logic controller membership functions: (**a**) ABS λ input; (**b**) ABS μ_x input; (**c**) ESP ψ input; (**d**) ESP δ input; (**e**) ABS p_{ABS} output; (**f**) ESP p_{ESPl} and p_{ESPr} outputs.

The μ_x MFs are plotted in Figure 5b. The UOD parameterization was obtained during the case study. The μ_x operational space is bounded between [10, 40].

The first input of the ESP FLC is the yaw rate. The state consists of nine MFs; UOD is limited in the range between [−4, 4] and introduced in Figure 5c. The reason behind the range for the UOD is next: when the angular velocity exceeds 4 rad/s and the steering wheel angle change is not conducted, vehicle spin appears and the driver is no longer able to act on lateral control.

The second input of the ESP steering wheel angle MFs is shown in Figure 5d. Like the first input, it has nine symmetrically dispelled MFs that are normalized between [−180, 180]. It is assumed that driver reaction in extreme situation must be limited to half of one full steering wheel turn to each side, left or right, which gives in total 360°.

The maximum pressure of the braking system for the studied case is 151 bar. The UOD for the output pressure variables (Figure 5e) is therefore located between [0, 151] and consists of eight MFs. The FLC decides how many bars shall be provided to obtain an optimal slip. Finally, the pressure output for the ESP is obtained in Figure 5f. Likewise, for the ABS the UOD lay between [0, 151]. The ESP has two outputs (Figure 4): brake pressure for the left and the right sides. The decision of which side of the vehicle to control is determined by the rule-base operator.

The modus ponens (If–Then) form has been used in this paper for the rule-base design. The multiple input, single output (MISO) form of the linguistic rules for ABS is (taken from [6]):

$$\textbf{If } u_1 \text{ is } A^j{}_1 \textbf{ and } u_2 \text{ is } A^k{}_2 \ldots \textbf{ Then } y_q \text{ is } B^p{}_q, \tag{10}$$

where u_1 and u_2 denote the FLC inputs wheel slip and road condition, respectively; y_q denotes the brake pressure; $A^j{}_1$ and $A^k{}_2$ relate to the jth and kth linguistic value associated with λ and μ_x, respectively; and $B^p{}_q$ is the linguistic value of the output braking pressure.

Linguistic values for the ABS are expressed in Table 3. There are 54 rules for the ABS control in total. The rule base for the ESP is observable in Table 4. It has a multi input, multi output (MIMO) structure. In total, 81 rules are required to control the state. The controlled side of the vehicle depends on the yaw moment direction from the center line of the car.

Table 3. Fuzzy linguistic rules for the ABS control.

μ_x \ λ	$\mathbf{MF_1}$	$\mathbf{MF_2}$	$\mathbf{MF_3}$	$\mathbf{MF_4}$	$\mathbf{MF_5}$	$\mathbf{MF_6}$	$\mathbf{MF_7}$	$\mathbf{MF_8}$	$\mathbf{MF_9}$
$\mathbf{MF_1}$	MF_2	MF_1	MF_1	MF_1	MF_1	MF_1	MF_1	MF_1	MF_1
$\mathbf{MF_2}$	MF_4	MF_3	MF_2	MF_1	MF_1	MF_1	MF_1	MF_1	MF_1
$\mathbf{MF_3}$	MF_6	MF_5	MF_4	MF_3	MF_2	MF_1	MF_1	MF_1	MF_1
$\mathbf{MF_4}$	MF_8	MF_7	MF_6	MF_5	MF_4	MF_3	MF_2	MF_1	MF_1
$\mathbf{MF_5}$	MF_8	MF_8	MF_8	MF_7	MF_6	MF_5	MF_3	MF_1	MF_1
$\mathbf{MF_6}$	MF_8	MF_8	MF_8	MF_8	MF_8	MF_7	MF_5	MF_3	MF_1

Table 4. Fuzzy linguistic rules for the ESP regulation: blue—left side of the vehicle, black—right side of the vehicle.

δ \ ψ	$\mathbf{MF_1}$	$\mathbf{MF_2}$	$\mathbf{MF_3}$	$\mathbf{MF_4}$	$\mathbf{MF_5}$	$\mathbf{MF_6}$	$\mathbf{MF_7}$	$\mathbf{MF_8}$	$\mathbf{MF_9}$
$\mathbf{MF_1}$	MF_1 / MF_1	MF_2	MF_2	MF_3	MF_3	MF_4	MF_4	MF_5	MF_5
$\mathbf{MF_2}$	MF_2	MF_1 / MF_1	MF_2	MF_2	MF_3	MF_3	MF_4	MF_4	MF_5
$\mathbf{MF_3}$	MF_2	MF_2	MF_1 / MF_1	MF_2	MF_2	MF_3	MF_3	MF_4	MF_4
$\mathbf{MF_4}$	MF_3	MF_2	MF_2	MF_1 / MF_1	MF_2	MF_2	MF_3	MF_3	MF_4
$\mathbf{MF_5}$	MF_3	MF_3	MF_2	MF_2	MF_1 / MF_1	MF_2	MF_2	MF_3	MF_3
$\mathbf{MF_6}$	MF_4	MF_3	MF_3	MF_2	MF_2	MF_1 / MF_1	MF_2	MF_2	MF_3
$\mathbf{MF_7}$	MF_4	MF_4	MF_3	MF_3	MF_2	MF_2	MF_1 / MF_1	MF_2	MF_2
$\mathbf{MF_8}$	MF_5	MF_4	MF_4	MF_3	MF_3	MF_2	MF_2	MF_1 / MF_1	MF_2
$\mathbf{MF_9}$	MF_5	MF_5	MF_4	MF_4	MF_3	MF_3	MF_2	MF_2	MF_1 / MF_1

For further fuzzy inference, Mamdani's method is applied in this paper. The last step in every FLC design is the defuzzification procedure. Relying on experience and due to the good computational complexity, the ABS is defuzzified by the centroid and the ESP by the smallest-of-maxima methods.

When all the design steps are finished, the rule base FLC can be expressed in a three-dimensional surface form. The ABS FLC for the front wheels is presented in Figure 6, whereas the ESP FLC for the left side of the vehicle surface is shown in Figure 7.

The ABS algorithm controls the slip by acting on the breaking pressure of each wheel. The ESP stabilizes the yaw rate by influencing the braking pressure with subtraction from the pressure generated for the ABS control. Table 5 summarizes the FLC design in this work.

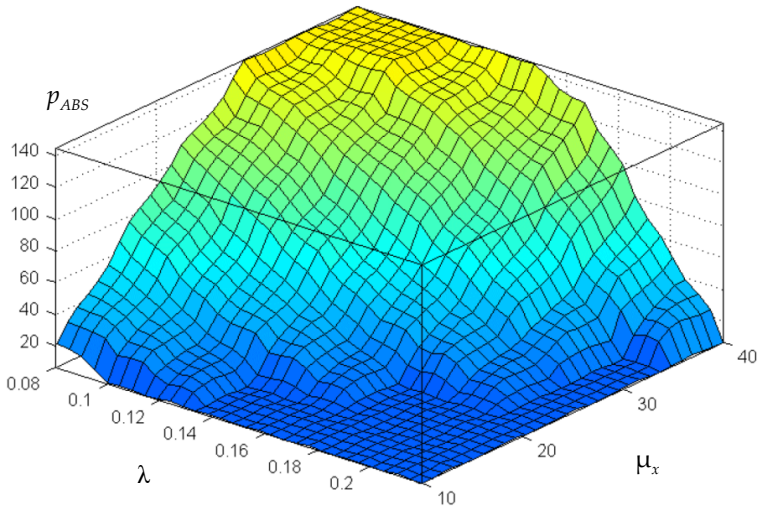

Figure 6. ABS FLC rule surface for the front wheels.

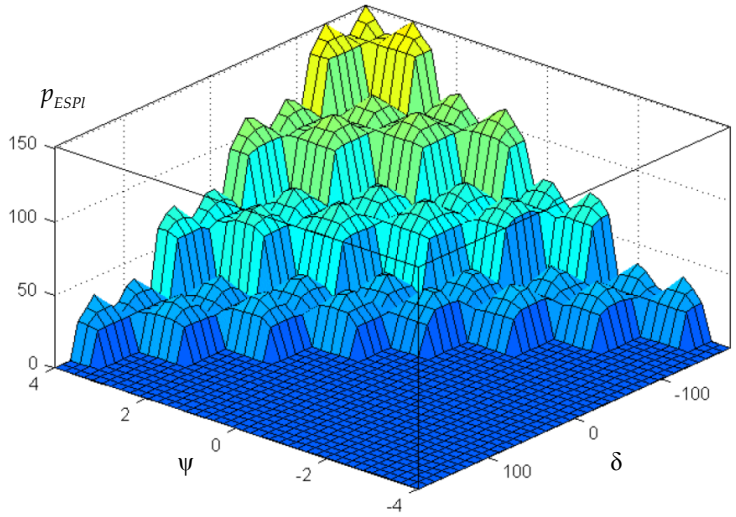

Figure 7. ESP FLC rule surface for the left side of the vehicle.

Table 5. Fuzzy logic controller design conclusion.

Parameter	ABS FLC	ESP FLC
Structure	MISO	MIMO
Crisp input	Slip λ (9 MFs), Road condition μ_x (6 MFs)	Yaw rate ψ (9 MFs), Steering wheel angle δ (9 MFs)
Crisp output	Braking pressure p_{ABS} (8 MFs)	Braking pressure left side p_{ESPl} (5 MFs), Braking pressure right side p_{ESPr} (5 MFs)
Fuzzy conjunction	AND = *min* (λ, μ_x)	AND = *min* (ψ, δ)
MFs	Linear Symmetric	Linear Symmetric
Inference method	Mamdani´s	Mamdani´s
Rule-base	54 Modes Ponens	81 Modes Ponens
Implication operation	*min* (p_{ABS})	*min* (p_{ESPl}) ∨ *min* (p_{ESPr})
Aggregation method	*max* (p_{ABS})	*max* (p_{ESPl}) ∨ *max* (p_{ESPr})
Defuzzification	Geometric center	Smallest-of-maxima

4. Simulation Conditions

The control algorithm is designed in Automotive Simulation Models™ (ASM) provided by the dSPACE® GmbH Software 2014-B (64-bit, Paderborn, Germany) and interacted with the MATLAB®/Simulink® R2013b (64 Bit, Natick, MA, USA). The ASM allows the multibody vehicle simulation procedures. The car model has 10 DOF. An overall software interface is presented in Figure 8.

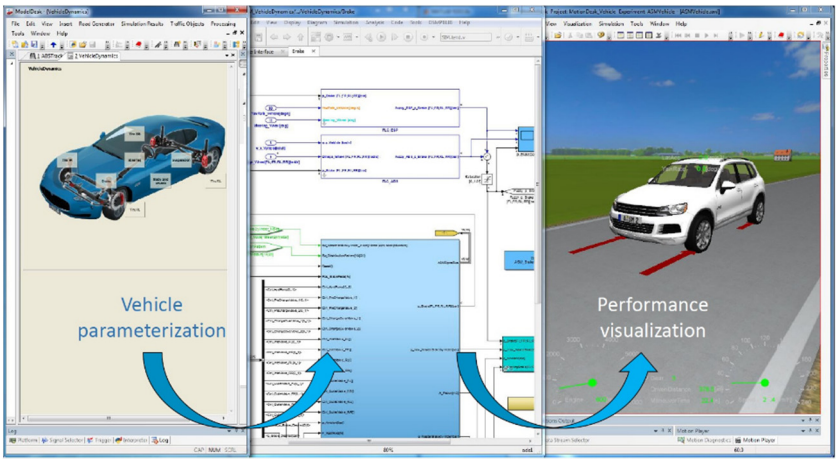

Figure 8. Simulation software interface by the dSPACE® GmbH.

During the simulation, the braking processes were conducted on a straight road as well as in combination with cornering maneuvers. Different complex maneuvers, such as straight or cornering braking on a split-μ road surface and straight or cornering with change of the tire–road friction coefficients, were simulated. The results are introduced as a comparison of the vehicle motion with and without the activated controllers. Road variations such as dry, wet, and icy surfaces as well as their combinations were designed and simulated to prove the ABS controller robustness and its ability to hold the optimal wheel slip in different road conditions.

The reaction of the ABS controller on the wheel slip characterizes the system adaptability. The factor can be expressed in percentage and calculated by the following equation:

$$\omega_{p-t-p} = \frac{\omega_{\max} - \omega_{\min}}{\omega_{\max}} \cdot 100. \tag{11}$$

Furthermore, the effect of the ABS controller performance can be described with the index of performance ABS_{IP}. The variable is a ratio between the vehicle deceleration with and without the controller and is found as follows:

$$ABS_{IP} = \frac{-a_{ABS}}{-a_{skid}}. \tag{12}$$

First, the simulation is dedicated to split-μ roads. When half of the road has a significantly higher friction coefficient as compared to the other half, a high yaw moment occurs. The driver is not able to compensate properly for the yaw dynamics, and the vehicle can spin around the COG. The corresponding simulation in this study is performed for cornering and straight braking maneuvers.

For the straight road, half wet–half dry and half icy–half wet surfaces were chosen. For the curved road, half dry–half icy and half wet–half dry surface profiles were designed.

Next, the model was simulated on a curved road line for different tire–road friction characteristics. The road friction conditions vary during the braking process from icy and dry to wet. Afterwards, the same road conditions were applied to the straight road profile. In this experimentation part the controller robustness is studied.

5. Results

5.1. Study on Controller Functionality

The first part of the simulation experiments is addressed to the vehicle safety investigation on the split-μ surface profiles. The maneuvers are simulated on straight and curved roads. For the straight braking, the vehicle was accelerated to 100 km/h and after that the emergency braking was conducted. For curved road braking the vehicle was accelerated to 65 km/h while the transport is cornering left.

Braking on a curved road with a split-μ surface is the most extreme situation for vehicle safety, because the yaw rate is created by the driver while cornering. The left side of the road is dry and the right side is icy in the present instance. The vehicle body and the wheel speed curves are shown in Figure 9.

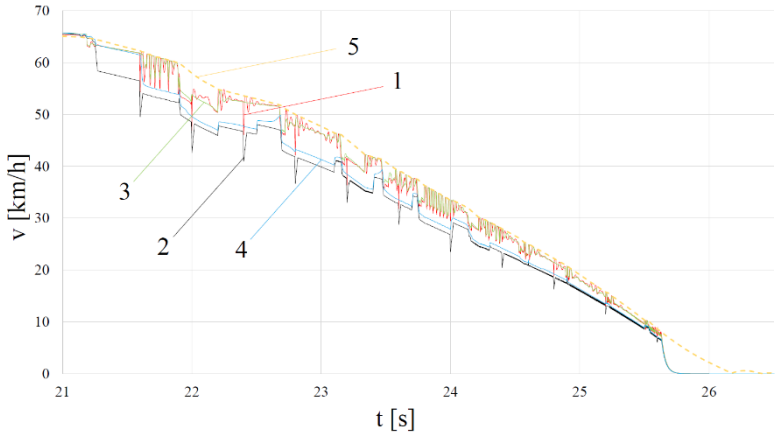

Figure 9. Braking on a curved split-μ road with a half dry–half icy surface; velocity profile curves: 1—FL wheel velocity, 2—FR wheel velocity, 3—RL wheel velocity, 4—RR wheel velocity, 5—vehicle velocity.

Before the ABS is activated, the ESP is already reducing the braking pressure from the left side of the vehicle (the dry surface). The slip values of the left side wheels are therefore lower compared to the right side (Figure 10). Although the left side of the road is dry, the left wheels have less than 10% of the wheel slip values, because the ESP reduces the braking pressure from the left half of the vehicle. The driver, thus, is able to control the car path to follow the road.

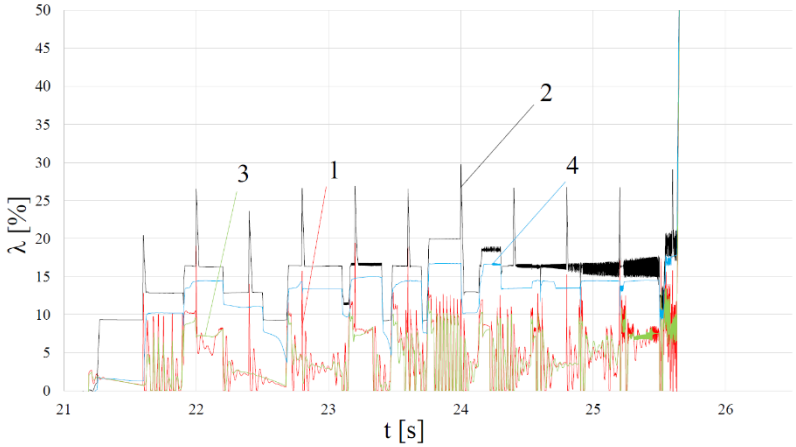

Figure 10. Braking on a curved split-μ road with a half dry–half icy surface; slip profile curves: 1—FL wheel slip, 2—FR wheel slip, 3—RL wheel slip, 4—RR wheel slip.

The dry surface has a higher friction coefficient than the icy road. In this case, the yaw rate is extremely high due to the left cornering. The yaw rate grows after the start of the braking process (Figure 11). However, the ESP reacts very fast and the braking pressure is minimized rapidly. Therefore, the yaw rate remains almost zero during the whole braking distance on the cornering maneuvers. Hence, the driver is able to maintain lateral stability during emergency braking.

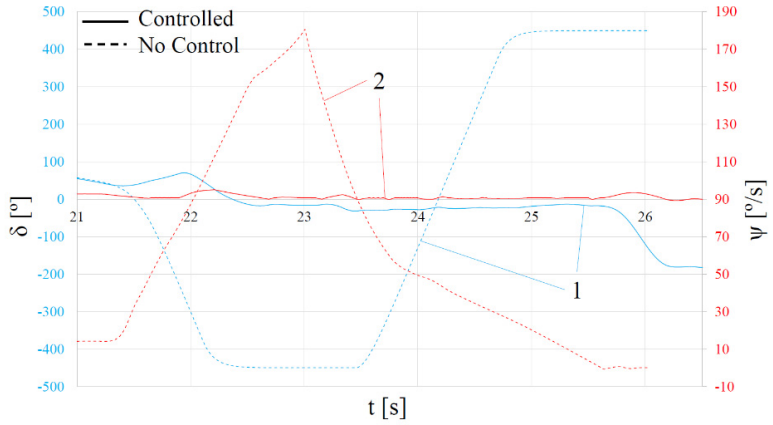

Figure 11. Braking on a curved split-μ road with a half dry–half icy surface profile angle curves: 1—steering wheel angle δ, 2—yaw rate ψ.

When the controller is switched off (Figure 11, dashed lines), the vehicle spins left. The driver turns the steering wheel to the right until the maximum allowed angle. Nevertheless, the high yaw rate in the opposite direction makes the car spin.

The simulation results with other split-μ road maneuvers are introduced in Table 6, the plots are represented in Figures S1–S9. The ESP safety assistance performance is also compared to the same condition simulations with the turned-off controller. The maximum yaw rate ψ_{max} does not exceed 26°/s. When the controller is turned off the yaw rate is very high, which makes the car spin around its COG even if the driver tries to keep the vehicle following the road. The braking distance s and the average body deceleration $-a_{average}$ for no control simulation are not introduced in the table, because in every case, when the controller is turned off, the car spins.

Table 6. Controller functionality results.

Criterion / Type	Braking Performance		ABS Control Performance			ESP Control Performance	
	s (m)	$-a_{average}$ (m/s^2)	$\lambda_{average}$ (%)		$\omega_{p\text{-}t\text{-}p}$ (%)	δ_{max} (°) Controlled/ No Control	ψ_{max} (°/s) Controlled/ No Control
Straight split-μ wet/dry	47.16	−4.25	FL FR RL RR	18.41 13.97 14.20 14.20	46.91 46.10 45.37 45.61	175.00/449.96	−16.86/−268.52
Straight split-μ icy/wet	102.51	−3.31	FL FR RL RR	12.74 7.34 10.62 5.10	32.51 27.63 24.85 18.15	60.16/450	−7.08/−313.73
Cornering split-μ dry/icy	44.74	−3.14	FL FR RL RR	4.71 15.96 4.40 13.05	28.26 35.04 23.24 28.58	−182.46/−450	25.49/−180.71
Cornering split-μ wet/dry	20.19	−5.23	FL FR RL RR	19.29 14.32 17.30 13.77	49.36 46.95 48.16 46.49	363.52/450	−15.42/−78.78

In short, the comparison simulation, where the controller was turned on and turned off, shows the importance of the proposed solution in terms of vehicle safety. Different complex maneuvers were studied. The driver is able to remain on the road, following the path. When the controller is turned off, steering is impossible and, the vehicle starts to spin around the COG, causing unfortunate car accidents.

5.2. Study on Controller Robustness

The next simulation study is devoted to an investigation of the controller robustness on curved and straight road profiles. The road surfaces are even. However, they are different for the whole braking distance. Again, in cornering maneuvers the vehicle is accelerated to 65 km/h in a straight line—to 100 km/h. Afterwards, emergency braking is performed.

The vehicle body and the vehicle wheels velocity plots for the varying road conditions on a straight road maneuvers are introduced in Figure 12. The vehicle starts braking on a dry road with transition to a wet surface. The car finishes braking on icy asphalt. The vehicle changes the deceleration according to the tire–road adhesive characteristics. The algorithm is able to recognize the road surface and, according to the obtained information supply, appropriate pressure to maintain efficient braking is applied.

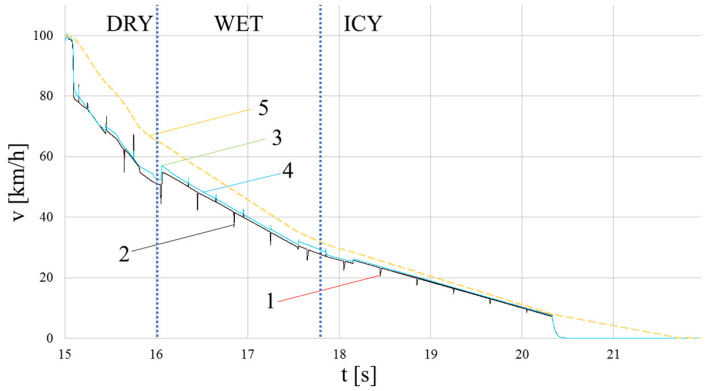

Figure 12. Braking on a straight road with dry–wet–icy surfaces profile speed curves: 1—FL wheel velocity, 2—FR wheel velocity, 3—RL wheel velocity, 4—RR wheel velocity, 5—vehicle velocity.

The slip curves for the each wheel are shown in Figure 13. No wheel lock has been obtained. The controller holds the optimal slip for each wheel on every road surface. The wheel pressure distribution aims to obtain an optimal wheel slip.

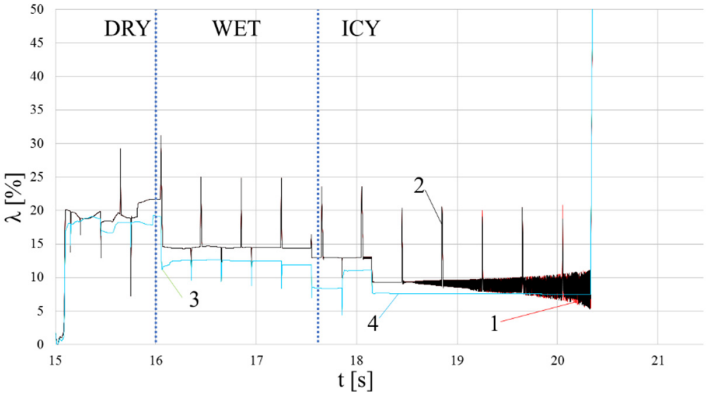

Figure 13. Braking on a straight road with dry–wet–icy surfaces profile slip curves: 1—FL wheel slip, 2—FR wheel slip, 3—RL wheel slip, 4—RR wheel slip.

Other braking results for the maneuvers with even road profiles studied in this paper are introduced in Figures S10–S17. To conclude the wheel slip control robustness and compare it to the theoretical energy efficient values from Figure 2, Table 7 is introduced. The simulation wheel slip results are taken as the average numbers. It can be concluded that the controller is able to maintain the optimal slip to maintain energy-efficient braking.

Table 7. Controller robustness results.

Criterion / Type	Braking Performance		ABS Control Performance			ESP Control Performance	
	s (m) Controlled/ No Control	$-a_{average}$ (m/s^2) Controlled/ No Control	ABS_{IP}	$\lambda_{average}$ (%)	$\omega_{p\text{-}t\text{-}p}$ (%)	δ_{max} (°) Controlled/ No Control	ψ_{max} (°/s) Controlled/ No Control
Cornering even wet to dry	21.59/30.88	−6.75/−3.48	1.94	FL 11.45–16.62 FR 14.27–17.79 RL 9.94–16.94 RR 11.61–17.90	34.76 37.88 32.93 35.44	103.55/450	10.82/−27.89
Cornering even dry to icy to wet	31.28/31.33	−3.69/−2.99	1.23	FL 19.14–3.68–9.918 FR 19.93–9.30–11.07 RL 17.34–2.94–8.93 RR 17.85–1.37–11.16	50.25 50.96 48.04 48.86	160.05/450	10.61/−20.72
Straight even icy to dry to wet	88.49/140.04	−4.29/−2.36	1.82	FL 10.01–18.99–14.16 FR 18.49–18.99–14.13 RL 7.73–17.13–12.33 RR 7.73–17.13–12.33	28.64 28.64 19.58 19.59	0/0	0/0
Straight even dry to wet to icy	62.51/140.04	−3.85/−1.97	1.95	FL 19.71–14.24–9.30 FR 19.71–14.24–9.30 RL 18.05–11.56–7.68 RR 18.05–11.56–7.68	55.66 55.66 48.52 48.53	0/0	0/0

In cornering maneuvers, as the vehicle is turning left, the wheel slip values for the left side of the vehicle are smaller compared to the right side. The difference is caused by the ESP assistance. In addition, even when the road surface is even, the yaw rate appears when the vehicle starts to brake. However, the driver reacts by controlling the steering wheel and the car remains on the road. Therefore, the robustness of the proposed controller is investigated through several examples of different complex maneuvers.

The braking and ESP performance results on the same roads without controllers are also introduced in Table 7. It is clear that the braking distances without the controllers are longer for every considered case. Due to the wheels' blockage, the average deceleration results ($-a_{average}$) are lower.

When the controllers are turned off, the driver rotates the steering wheel as far as possible to remain on the road while conducting the cornering maneuvers. The car, however, drives off the road without controller assistance. When the controllers are turned on, contrariwise, it is enough for the driver to slightly control the vehicle steering wheel to remain on the road.

All in all, the ABS FLC is able to recognize the tire–road adhesive coefficient and supply the appropriate braking pressure to maintain energy-efficient deceleration. The simulation results of the controller on the straight and cornering profiles prove the controller's robustness.

6. Discussion and Conclusions

This paper describes the FLC algorithm for vehicle safety assistance control. The ABS and the ESP integration introduced in this work provides energy-efficient and robust responses to different road surfaces and curved braking performance. In order to design a robust FLC, the tire–road adhesive coefficients versus tire slip curves for dry, damp, wet, and icy roads were plotted first (Figure 2). The studied vehicle model was parameterized according to the SUV parameters. The proposed solution is suitable for the studied SUV model.

A combination of ABS and ESP controllers both based on FLC theory is introduced. Each wheel has an independent controller. The simulation results conducted on different complex maneuvers

involving curved road profiles and split-μ road surfaces as well as varying road friction coefficients prove the controller robustness. The algorithm assists the driver with steering. Thus, a driver with average reaction times is able to follow the road during emergency heavy braking.

The simulation results introduced in Section 5 prove the FLC robustness to varying road surfaces and split-μ profiles. Moreover, optimal slip braking on even road profiles is maintained, providing energy-efficient braking. Comparing the research results to other intelligent computation control algorithms introduced in Section 1, the current study offers several novel proposals for the vehicle dynamics and safety control fields.

First, the proposed controller does not require a reference error and change of error input variables as in [10–12,15] Instead, the controller covers the whole braking process stable area. The human experience containing rule-base block provides a suitable pressure to hold an optimal for every studied road surface slip value. Therefore, the dependence on the constant reference value, which is unpredictable in reality, is avoided.

Second, in most of the previously proposed cases, as for instance in [10–12,16], braking on a straight even surface excludes the lateral dynamics influence on the controller, and, thus, on the vehicle safety performance. The simulation results in Section 5 show that the lateral dynamics during cornering maneuvers and on split-μ road profiles braking must be taken into consideration as they are essential in car spin and roll-over avoidance. Otherwise, the ABS and ESP safety assistance cannot be ensured.

Third, the simple quarter-car model studied in [9,18] is not enough to prove the controller productivity and robustness. In reality, the four-wheel vehicle model represents a more complex control task. Consequently, the vehicle model examined in this paper has an advantage over other similar works.

Finally, regarding the ESP performance, most researchers [20,21,23–25] limit their results with a simple line change maneuver. There were no publications found testing the ABS and ESP designed with FLC on a cornering split-μ road profile, as has been done in the current work.

In short, the results obtained from the current research are as follows:

- The ESP and ABS FLC control integration to obtain energy-efficient braking performance.
- The controls safety and robustness in different kinds of complex maneuvers is studied.
- Use of a complex 10 DOF vehicle model in the controller simulation.

The main drawback of the presented work, however, is its restriction by the numerical simulation. In the PC software simulation, the real vehicle dynamics and physical behavior are missing. A computer simulation does not completely solve the problem.

Future research covers the experimentation on the HIL brakes test bench. Moreover, the controller will be designed and applied on a four in-wheel-motor drive passenger electric vehicle providing the torque-base brake solution to study recuperative braking.

Supplementary Materials: The following are available online at www.mdpi.com/2076-3417/6/12/382/s1, Figure S1: Straight split-μ road with a half wet-half dry surface profile velocity curves, Figure S2: Straight split-μ road with a half wet-half dry surface profile wheel slip curves, Figure S3: Straight split-μ road with a half wet-half dry surface profile angle curves, Figure S4: Straight split-μ road with a half icy-half wet surface profile velocity curves, Figure S5: Straight split-μ road with a half icy-half wet surface profile wheel slip curves, Figure S6: Straight split-μ road with a half icy-half wet surface profile angle curves, Figure S7: Curved split-μ road with a half wet-half dry surface profile velocity curves, Figure S8: Curved split-μ road with a half wet-half dry surface profile wheel slip curves, Figure S9: Curved split-μ road with a half wet-half dry surface profile angle curves, Figure S10: Curved even road with wet-dry surface profile velocity curves, Figure S11: Curved even road with wet-dry surface profile wheel slip curves, Figure S12: Curved even road with wet-dry surface profile angle curves, Figure S13: Curved even road with dry-icy-wet surface profile velocity curves, Figure S14: Curved even road with dry-icy-wet surface profile wheel slip curves, Figure S15: Curved even road with dry-icy-wet surface profile angle curves, Figure S16: Straight even road with icy-dry-wet surface profile velocity curves, Figure S17: Straight even road with icy-dry-wet surface profile wheel slip curves.

Acknowledgments: This research work was supported by the Deutschen Bundesstiftung Umwelt (DBU) exchange scholarship program and the European Union's Horizon 2020 research and innovation programme under the

Marie Skłodowska-Curie grant agreement No 645736. We acknowledge support for the Article Processing Charge from the German Research Foundation and the Open Access Publication Fund of the Technische Universität Ilmenau.

Author Contributions: Andrei Aksjonov conceived designed and performed the experiments. Klaus Augsburg and Valery Vodovozov analyzed the data; all the authors prepared the manuscript.

Conflicts of Interest: The authors declare no conflict of interest.

References

1. Post, W.; Koch-Dücker, H.-J.; Papert, U. Car braking systems. Antilock braking system. In *Brakes, Brake Control and Driver Assistance Systems: Function, Regulation and Components*; Reif, K., Ed.; Springer: Friedrichshafen, Germany, 2014; pp. 28–40, 74–94.
2. Ivanov, V. A review of fuzzy methods in automotive engineering applications. *Eur. Transp. Res. Rev.* **2015**, *7*, 1–10. [CrossRef]
3. Takahashi, H.; Ishikawa, Y. Antiskid Brake Control System Based on Fuzzy Inference. U.S. Patent 4,842,344, 27 June 1989.
4. Mauer, G.F. A fuzzy logic controller for an ABS braking system. *IEEE Trans. Fuzzy Syst.* **1998**, *3*, 381–388. [CrossRef]
5. Klaus, K.; Hasemann, M. An embedded fuzzy anti-slippage system for heavy duty off road vehicles. *Inf. Sci.* **1995**, *4*, 1–27. [CrossRef]
6. Passino, K.M.; Yurkovich, S. *Fuzzy Control*; Addison Wesley Longman, Inc.: Menlo Park, California, CA, USA, 1998; pp. 317–413.
7. Layne, J.R.; Passino, K.M.; Yurkovich, S. Fuzzy learning control for antiskid braking systems. *IEEE Trans. Control Syst. Technol.* **1993**, *2*, 122–129. [CrossRef]
8. Dai, C.L.; Xu, L.J. The Simulation Research of Automobile ABS System Based on Fuzzy Theory. In Proceedings of the 2015 International Conference on Intelligent Transportation, Big Data and Smart City (ICITBS), Halong Bay, Vietnam, 19–20 December 2015; pp. 922–926.
9. Du, H.; Li, W.; Zhang, Y. Tracking Control of Wheel Slip Ratio with Velocity Estimation for Vehicle Anti-Lock Braking System. In Proceedings of the 2015 27th Chinese Control and Decision Conference (CCDC), Qingdao, China, 23–25 May 2015; pp. 1900–1905.
10. Raesian, N.; Khajehpour, N.; Yaghoobi, M. A New Approach in Anti-lock Braking System (ABS) Based on Adaptive Neuro-Fuzzy Self-tuning PID Controller. In Proceedings of the 2011 2nd International Conference on Control, Instrumentation and Automation (ICCIA), Shiraz, Iran, 27–29 December 2011; pp. 530–535.
11. Kejun, J.; Chengye, L. Application Study of Fuzzy PID Control with S-function on Automotive ABS. In Proceedings of the 2010 International Conference on Future Information Technology and Management Engineering (FITME), Changzhou, China, 9–10 October 2010; pp. 467–470.
12. Jidu, H.; Yongjun, Z.; Gang, W. Research on Vehicle Anti-braking System Control Algorithm Based on Fuzzy Immune Adaptive PID Control. In Proceedings of the 2012 Third International Conference on Digital Manufacturing and Automation (ICDMA), Guilin, China, 31 July–2 August 2012; pp. 723–726.
13. Lin, C.-M.; Li, H.-Y. Intelligent hybrid control system design for antilock braking systems using self-organizing function-link fuzzy cerebellar model articulation controller. *IEEE Trans. Fuzzy Syst.* **2013**, *21*, 1044–1055. [CrossRef]
14. Mirzaei, A.; Moallem, M.; Dehkordi, B.M.; Fahimi, B. Design of an optimal fuzzy controller for antilock braking system. *IEEE Trans. Vehicul. Technol.* **2006**, *55*, 1725–1730. [CrossRef]
15. Yonggon, L.; Zak, S.H. Designing a genetic neural fuzzy antilock-brake-system controller. *IEEE Trans. Evol. Comp.* **2002**, *6*, 198–211. [CrossRef]
16. Wang, W.-Y.; Li, I.H.; Chen, M.-C.; Su, S.-F.; Hsu, S.-B. Dynamic slip-ratio estimation and control of antilock braking systems using an observer-based direct adaptive fuzzy-neural controller. *IEEE Trans. Ind. Electron.* **2009**, *56*, 746–1756.
17. Cabrera, J.A.; Ortiz, A.; Castello, J.J.; Simon, A. A fuzzy logic control for antilock braking system integrated in the IMMa tyre test bench. *IEEE Trans. Veh. Technol.* **2005**, *54*, 1937–1949. [CrossRef]
18. Khatun, P.; Bingham, C.M.; Schofield, N.; Mellor, P.H. Application of fuzzy control algorithms for electric vehicle antilock braking-traction control systems. *IEEE Trans. Veh. Technol.* **2003**, *52*, 1356–1364. [CrossRef]

19. Cao, C.-T.; Becker, R.; Belzner, U.; Moeller, T.-W.; Lieberoth-Leden, B. System for Controlling Brake Pressure Based on Fuzzy Logic Using Steering Angle and Yaw Speed. U.S. Patent 5,634,698, 3 June 1997.
20. Zhou, H.; Chen, H.; Ren, B.; Zhao, H. Yaw Stability Control for In-wheel-motored Electric Vehicle with a Fuzzy PID Method. In Proceedings of the 27th Chinese Control and Decision Conference (2015 CCDC), Qingdao, China, 23–25 May 2015; pp. 1876–1881.
21. Wei, Z.; Guizhen, Y.; Jian, W.; Tianshu, S.; Xiangyang, X. Self-tuning Fuzzy PID Applied to Direct Yaw Moment Control for Vehicle Stability. In Proceedings of the 9th International Conference on Electronic Measurement & Instruments, 2009, (ICEMI '09), Beijing, China, 16–19 August 2009; pp. 2-257–2-261.
22. Tahami, F.; Kazemi, R.; Farhanghi, S. A novel driver assist stability system for all-wheel-drive electric vehicle. *IEEE Trans. Vehicul. Technol.* **2003**, *52*, 683–692. [CrossRef]
23. Geng, C.; Mostefai, L.; Denai, M.; Hori, Y. Direct yaw-moment control of an in-wheel-motored electric vehicle based on body slip angle fuzzy observer. *IEEE Trans. Ind. Electron.* **2009**, *56*, 1411–1419. [CrossRef]
24. Oudghiri, M.; Chadli, M.; Hajjaji, A.E. Vehicle Yaw Control Using a Robust H∞ Observer-based Fuzzy Controller Design. In Proceedings of the 2007 46th IEEE Conference on Decision and Control, New Orleans, LA, USA, 12–14 December 2007; pp. 3895–3900.
25. Wu, Y.; Song, D.; Hou, Z.; Yuan, X. A Fuzzy Control Method to Improve Vehicle Yaw Stability Based on Integrated Yaw Moment Control and Active Front Steering. In Proceedings of the 2007 International Conference on Mechatronics and Automation, Harbin, China, 5–8 August 2007; pp. 1508–1512.